

CrystEngComm

Accepted Manuscript



This is an *Accepted Manuscript*, which has been through the Royal Society of Chemistry peer review process and has been accepted for publication.

Accepted Manuscripts are published online shortly after acceptance, before technical editing, formatting and proof reading. Using this free service, authors can make their results available to the community, in citable form, before we publish the edited article. We will replace this *Accepted Manuscript* with the edited and formatted *Advance Article* as soon as it is available.

You can find more information about *Accepted Manuscripts* in the [Information for Authors](#).

Please note that technical editing may introduce minor changes to the text and/or graphics, which may alter content. The journal's standard [Terms & Conditions](#) and the [Ethical guidelines](#) still apply. In no event shall the Royal Society of Chemistry be held responsible for any errors or omissions in this *Accepted Manuscript* or any consequences arising from the use of any information it contains.

Cite this: DOI: 10.1039/c0xx00000x

www.rsc.org/xxxxxx

ARTICLE TYPE

Structural Diversity of Luminescent Lanthanide Metal-Organic Frameworks based on a V-Shaped Ligand

Yan-Fei He, Di-Ming Chen, Hang Xu and Peng Cheng*

Received (in XXX, XXX) XthXXXXXXXXX 20XX, Accepted Xth XXXXXXXXXXXX 20XX

DOI: 10.1039/b000000x

Four types of luminescent lanthanide metal-organic frameworks (Ln-MOFs) with the formulas $[\text{Ln}_2(\text{OBA})_3(\text{DMA})_2(\text{H}_2\text{O})_2]_n$ [**1**, Ln = Eu (**1-Eu**), Tb (**1-Tb**)], $\{[\text{Ln}_2(\text{OBA})_3(\text{H}_2\text{O})_4] \cdot 2\text{H}_2\text{O}\}_n$ [**2**, Ln = Eu (**2-Eu**), Tb (**2-Tb**)], $\{[\text{Ln}(\text{OBA})(\text{HOBA})(\text{H}_2\text{O})_2] \cdot 3\text{DMF}\}_n$ [**3**, Ln = Eu (**3-Eu**), Tb (**3-Tb**)], and $[\text{Ln}_2(\text{OBA})_3(\text{DMF})(\text{H}_2\text{O})_2]_n$ [**4**, Ln = Eu (**4-Eu**), Tb (**4-Tb**)] ($\text{H}_2\text{OBA} = 4,4'$ -oxybis(benzoate) acid, DMA = N,N-dimethylacetamide, DMF = N,N-dimethylformamide), have been solvothermally synthesized based on a V-shaped ligand H_2OBA under different conditions. The structural features of the four types of Ln-MOFs are as follows: **1** shows 3D framework in which the dinuclear SBUs are further cross-linked by OBA^{2-} ligands. Both **2** and **3** exhibit 2D network constructed by 1D chain. **4** features a 2D network, in which 1D chains and dinuclear SBU arranged alternately through the OBA^{2-} ligands. **4** can be transformed to **3** at room temperature in mother solution. The experimental results reveal that solvent and temperature play important roles in constructing coordination polymers. All the aforementioned Ln-MOFs are fully characterized by elemental analysis, infrared spectroscopy, and thermogravimetric analysis. The luminescent properties of these Ln-MOFs have been studied, showing emission characteristic for inorganic species at room temperature.

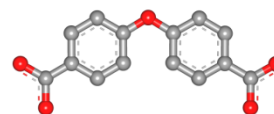
Introduction

In recent years, lanthanide metal-organic frameworks (Ln-MOFs) have attracted extensive attention due to their novel topological structures as well as potential applications in gas storage/separation,¹ catalysis,² luminescence,³ and magnetic properties.⁴ Compared to other MOF materials, Ln-MOFs exhibit an unique luminescent mechanism in which includes ligand-to-metal energy transitions arising from suitable “antenna effect”.⁵ As a result, Ln-MOFs involving Eu^{3+} and Tb^{3+} centres were widely investigated owing to their intense visible luminescence in the red and green regions and spectrally narrow emission as lumophores. On the other hand, in order to achieve the energy transitions, the selection of a suitable ligand containing chromophore to act as antenna is also important. In view of the reported studies, phenyl and pyridyl are good luminescent chromophores.⁶

According to the Pearson’s HSAB principle, lanthanide ions are considered as hard acids tend to link with hard donor atoms (such as oxygen),⁷ thus the aromatic multiple carboxylate ligands could be served as a good candidate in Ln-MOFs self-assembled. However, design and synthesis of desirable coordination frameworks are still a challenge because the resulting products are affected by a variety of factors such as reaction temperature, time, pH, molar ratio of reactants, central metal ions, solvent and so on.⁸ Sometimes small adjustment of one and more factors may

lead to a drastic change in the dimensionality and topology.⁹

In this article, we choose a V-shaped multiple carboxylate ligand 4,4'-oxybis(benzoate) acid (H_2OBA , Scheme 1) as the bridging ligand to investigate the role of reaction conditions in structural control of Ln-MOFs. Several 2D and 3D lanthanide metal-organic frameworks based on 4,4'-oxybis(benzoate) acid have been reported. For example, Lin *et al.* reported two 2D Ln-MOFs containing $\{\text{Ln}_2\}$ secondary unit¹⁰. Wang *et al.* prepared three 3D Ln-MOFs possessing $\{\text{Ln}_3\}$ or $\{\text{Ln}_6\}$ building block. However, a systematic research of solvent and temperature induced structural diversity still not be implemented¹¹. Four types of luminescent Ln-MOFs, namely $[\text{Ln}_2(\text{OBA})_3(\text{DMA})_2(\text{H}_2\text{O})_2]_n$ [**1**, Ln = Eu (**1-Eu**), Tb (**1-Tb**)], $\{[\text{Ln}_2(\text{OBA})_3(\text{H}_2\text{O})_4] \cdot 2\text{H}_2\text{O}\}_n$ [**2**, Ln = Eu (**2-Eu**), Tb (**2-Tb**)], $\{[\text{Ln}(\text{OBA})(\text{HOBA})(\text{H}_2\text{O})_2] \cdot 3\text{DMF}\}_n$ [**3**, Ln = Eu (**3-Eu**), Tb (**3-Tb**)], and $[\text{Ln}_2(\text{OBA})_3(\text{DMF})(\text{H}_2\text{O})_2]_n$ [**4**, Ln = Eu (**4-Eu**), Tb (**4-Tb**)] ($\text{H}_2\text{OBA} = 4,4'$ -oxybis(benzoate) acid, DMA = N,N-dimethylacetamide, DMF = N,N-dimethylformamide) have been synthesized and fully characterized. The luminescent properties of all Ln-MOFs have been studied, showing emission characteristic towards inorganic species at room temperature.



Scheme 1 V-shaped Dicarboxylate Ligand (H_2OBA) (H atoms are omitted for clarity)

Experimental

Materials and Measurements

All reagents and solvents were provided by commercial reagents company and used as received. Element Analysis for C, H, and N were performed on a Perkin Elmer 240 CHN elemental analyzer. IR spectra were measured in the range 400–4000 cm^{-1} on a Bruker TENOR 27 spectrophotometer by using KBr pellets. Powder X-ray diffraction measurements were collected on a Rigaku D/Max-2500 X-ray diffractometer using Cu K α radiation. Thermogravimetric analysis (TGA) were carried out a Labsys NETZSCH TG 209 Setaram apparatus with a heating rate of 10 $^{\circ}\text{C}/\text{min}$ in a nitrogen atmosphere in a temperature range 25–800 $^{\circ}\text{C}$. The solid luminescent spectra were recorded on a Varian Cary Eclipse Fluorescence spectrophotometer at room temperature.

Synthesis of Ln-MOFs 1-4

*Synthesis of $[\text{Ln}_2(\text{OBA})_3(\text{DMA})_2(\text{H}_2\text{O})_2]_n$ (**1**, Ln = Eu (**1-Eu**), Tb (**1-Tb**)).* The mixture of $\text{Ln}(\text{NO}_3)_3 \cdot 6\text{H}_2\text{O}$ (0.1 mmol), H_2OBA (0.1 mmol, 25.8 mg) and 4 mL $\text{DMA}/\text{H}_2\text{O}$ (1:1, v/v) was put into a Parr Teflon-lined stainless steel reactor (25 mL) under autogenous pressure and heated at 120 $^{\circ}\text{C}$ for 3 days, and then slowly cooled to room temperature in two days. Colourless plate-like crystals suitable for X-ray data collection were obtained. Yield: ca. **1-Eu** of 57% based on H_2OBA . Anal. Calcd (%) for **1-Eu** ($\text{C}_{50}\text{H}_{46}\text{N}_2\text{O}_{19}\text{Eu}_2$): C, 46.81; H, 3.61; N, 2.18. Found: C, 46.34; H, 3.37; N, 2.30. IR (KBr, cm^{-1}): 3420(s, br), 2026(w), 1598(s), 1540(m), 1412(s), 1258(m), 1115(vs), 883(m), 787(m), 616(s). Yield: ca. **1-Tb** of 69% based on H_2OBA . Anal. Calcd (%) for **1-Tb** ($\text{C}_{50}\text{H}_{46}\text{N}_2\text{O}_{19}\text{Tb}_2$): C, 46.31; H, 3.58; N, 2.16. Found: C, 46.34; H, 3.78; N, 2.42. IR (KBr, cm^{-1}): 3422(s, br), 2026(w), 1596(s), 1531(m), 1412(s), 1258(m), 1119(vs), 881(m), 785(m), 618(s).

*Synthesis of $\{[\text{Ln}_2(\text{OBA})_3(\text{H}_2\text{O})_4] \cdot 2\text{H}_2\text{O}\}_n$ (**2**, Ln = Eu (**2-Eu**), Tb (**2-Tb**)).* The mixture of $\text{Ln}(\text{NO}_3)_3 \cdot 6\text{H}_2\text{O}$ (0.1 mmol), H_2OBA (0.1 mmol, 25.8 mg) and 3 mL $\text{DMA}/\text{H}_2\text{O}$ (1:2, v/v) was sealed in a Parr Teflon-lined stainless steel reactor (25 mL) under autogenous pressure and heated at 120 $^{\circ}\text{C}$ for 3 days, and then slowly cooled to room temperature in two days. Block-shaped colourless crystals suitable for X-ray data collection were obtained. Yield: ca. **2-Eu** of 49% based on H_2OBA . Anal. Calcd (%) for **2-Eu** ($\text{C}_{42}\text{H}_{36}\text{O}_{21}\text{Eu}_2$): C, 42.73; H, 3.08. Found: C, 42.99; H, 3.53. IR (KBr, cm^{-1}): 3443(s, br), 2025(w), 1596(s), 1529(m), 1411(s), 1117(vs), 880(m), 621(s). Yield: ca. **2-Tb** ($\text{C}_{42}\text{H}_{36}\text{O}_{21}\text{Tb}_2$) of 42% based on H_2OBA . Anal. Calcd (%) for **2-Tb**: C, 42.23; H, 3.04. Found: C, 42.59; H, 3.45. IR (KBr, cm^{-1}): 3422(s, br), 1598(s), 1540(m), 1415(m), 1116(vs), 881(m), 618(s).

*Synthesis of $\{[\text{Ln}(\text{OBA})(\text{HOBA})(\text{H}_2\text{O})_2] \cdot 3\text{DMF}\}_n$ (**3**, Ln = Eu (**3-Eu**), Tb (**3-Tb**)).* The mixture of $\text{Ln}(\text{NO}_3)_3 \cdot 6\text{H}_2\text{O}$ (0.1 mmol), H_2OBA (0.1 mmol, 25.8 mg) and 4 mL $\text{DMF}/\text{H}_2\text{O}$ (1:1, v/v) was placed in sealed glass bottle and heated at 80 $^{\circ}\text{C}$ for 3 days, colourless block-like crystals suitable for X-ray data collection were obtained. Yield: ca. **3-Eu** of 65% based on H_2OBA . Anal. Calcd (%) for **3-Eu** ($\text{C}_{37}\text{H}_{42}\text{N}_3\text{O}_{15}\text{Eu}$): C, 48.27; H, 4.60; N, 4.56. Found: C, 48.27; H, 5.04; N, 4.27. IR (KBr, cm^{-1}): 3283 (br), 2930 (w), 2027 (m), 1704 (m), 1668 (s), 1596 (s), 1535(s), 1413(s), 1239(s), 1107(s), 879 (s), 790(s), 618(s). Yield: ca. **3-Tb** of 77% based on H_2OBA . Anal. Calcd for **3-Tb** ($\text{C}_{37}\text{H}_{42}\text{N}_3\text{O}_{15}\text{Tb}$):

C, 47.90; H, 4.56; N, 4.53. Found: C, 47.52; H, 4.77; N, 4.27. IR (KBr, cm^{-1}): 3383(s, br), 2930(w), 2025(m), 1704(m), 1670(s), 1596(s), 1541(s), 1415(s), 1238(s), 1101(s), 879(s), 790(s), 618(s).

*Synthesis of $[\text{Ln}_2(\text{OBA})_3(\text{DMF})(\text{H}_2\text{O})_2]_n$ (**4**, Ln = Eu (**4-Eu**), Tb (**4-Tb**)).* The mixture of $\text{Ln}(\text{NO}_3)_3 \cdot 6\text{H}_2\text{O}$ (0.2 mmol), H_2OBA (0.3 mmol, 77.4 mg), and 4 mL $\text{DMF}/\text{H}_2\text{O}$ (1:1, v/v) was put into a Parr Teflon-lined stainless steel reactor (25 mL) under autogenous pressure and heated at 120 $^{\circ}\text{C}$ for 3 days, and then slowly cooled to room temperature in two days, colourless Needle-like crystals suitable for X-ray data collection were collected. Yield: ca. **4-Eu** of 32% based on H_2OBA . Anal. Calcd (%) for **4-Eu** ($\text{C}_{45}\text{H}_{35}\text{NO}_{18}\text{Eu}_2$): C, 45.74; H, 2.99; N, 1.19. Found: C, 45.39; H, 3.11; N, 1.34. IR (KBr, cm^{-1}): 3422(s, br), 2026(m), 1597(s), 1543(m), 1411(s), 1254(m), 1161(s), 882(s), 785(s), 618(s). Yield: ca. **4-Tb** of 42% based on H_2OBA . Anal. Calcd for **4-Tb** ($\text{C}_{45}\text{H}_{35}\text{NO}_{18}\text{Tb}_2$): C 45.21, H 2.95, N 1.17. Found: C, 45.62; H, 3.23; N, 1.44. IR (KBr, cm^{-1}): 3395(s, br), 2027(m), 1596(s), 1543(m), 1414(s), 1239(m), 1162 (s), 881(s), 783(s), 618(s).

X-ray crystallography

Single-crystal X-ray data of Ln-MOFs **1**, **3** and **4** were collected on a Agilent Technologies SuperNova single-crystal diffractometer by using graphite-monochromatic Mo K α radiation ($\lambda = 0.71073$ Å). The structures were solved by direct methods and refined by full matrix least-squares techniques using SHELXS and SHELXL programs.¹² With anisotropic thermal factors for all non-hydrogen atoms and the hydrogen atoms were positioned geometrically, except for some disordered atoms. Several DFIX commands were used to fix the bond distances. For Ln-MOFs **1**, one benzene ring of the OBA²⁻ ligand was disordered with occupancy of 0.49:0.51, while the oxygen atom bridged two benzene rings and three carbon atoms of the other benzene ring was disordered with the same occupancy of 0.45:0.55 for two different positions. The coordinated DMA molecule was disordered with occupancy of 0.34:0.66. The selected crystal parameters and refinements are summarized in Table 1.

Results and discussion

Syntheses

All Ln-MOFs were synthesized in different reaction conditions by solvothermal methods. The resulting products of solvothermal methods are depended on many factors, such as reaction temperature, time, pH, molar ratio of reactants, and the solvent.⁹ Different synthesis conditions may lead different outcomes. The synthetic strategies of all Ln-MOFs are shown in Scheme 2. Comprehensive analysis of PXRD and elemental analysis indicate that **2** possess an isostructure as reported.¹³ The Ln-MOFs **2** presented here is to make a comparison and discussion for the control of the diversity in self-assembled of Ln-MOFs. Ln-MOFs **1-3** were synthesized by using the same starting material with different solvents and temperature. Ln-MOF **1** was solvothermally synthesized in $\text{DMA}/\text{H}_2\text{O}$ (volume ratio 1:1) solvent system. When the volume ratio was changed to 1:2, a 2D Ln-MOF (**2**), with 1D chain was formed. Obviously, the volume ratio ($\text{DMA}/\text{H}_2\text{O}$) played an important role in the formation of the resulting Ln-MOFs. When temperature was changed to 80 $^{\circ}\text{C}$ and

Table 1 Crystal data and structural refinement parameters of **1**, **3** and **4**

	1-Eu	1-Tb	3-Eu	3-Tb	4-Eu	4-Tb
Formula	C ₅₀ H ₄₆ N ₂ O ₁₉ Eu ₂	C ₅₀ H ₄₆ N ₂ O ₁₉ Tb ₂	C ₃₇ H ₄₂ N ₃ O ₁₅ Eu	C ₃₇ H ₄₂ N ₃ O ₁₅ Tb	C ₄₅ H ₃₅ NO ₁₈ Eu ₂	C ₄₅ H ₃₅ NO ₁₈ Tb ₂
Formula weight	1282.81	1296.73	919.69	927.66	1180.65	1195.58
Temperature/K	129.8(5)	130.4(2)	293(2)	130.30(14)	133.8(2)	129.6(2)
Crystal system	monoclinic	monoclinic	triclinic	triclinic	monoclinic	monoclinic
Space group	<i>C2/c</i>	<i>C2/c</i>	<i>P</i> $\bar{1}$	<i>P</i> $\bar{1}$	<i>P2</i> ₁ / <i>c</i>	<i>P2</i> ₁ / <i>c</i>
<i>a</i> (Å)	30.4852(10)	30.379(2)	9.4805(4)	9.3955(5)	9.4187(6)	9.3673(4)
<i>b</i> (Å)	9.0518(3)	8.9963(4)	13.8989(7)	13.8663(6)	28.0878(14)	27.9636(9)
<i>c</i> (Å)	20.1865(7)	20.1175(14)	16.6460(9)	16.5559(10)	16.7579(11)	16.8012(6)
α (°)	90.00	90.00	85.350(4)	85.363(4)	90.00	90.00
β (°)	107.086(3)	107.423(8)	76.570(4)	76.965(5)	99.446(6)	99.382(4)
γ (°)	90.00	90.00	72.158(5)	72.239(5)	90.00	90.00
<i>Z</i>	4	4	2	2	4	4
<i>V</i> (Å ³)	5324.5(3)	5245.9(6)	2030.70(18)	2001.02(19)	4373.2(5)	4342.1(3)
ρ calc.(g/cm ³)	1.600	1.642	1.504	1.540	1.793	1.829
μ (mm ⁻¹)	2.408	2.750	1.615	1.839	2.922	3.311
<i>F</i> (000)	2552.0	2568.0	934.0	940.0	2324.0	2344.0
θ min–max (°)	5.94 to 50.02	5.72 to 50.02	5.72 to 50.02	5.76 to 50.02	5.56 to 50.02	5.58 to 50.02
Reflns collected	20344	11976	14085	14824	18345	19812
Independent reflns	4687	4615	7148	7050	7618	7568
<i>R</i> (int)	0.0485	0.0433	0.0345	0.0407	0.0378	0.0341
<i>S</i>	1.036	1.047	1.063	1.054	1.034	1.080
<i>R</i> ₁ , <i>wR</i> ₂ (<i>I</i> > 2 σ (<i>I</i>)) ^a	0.0485, 0.1256	0.0794, 0.2103	0.0331, 0.0790	0.0308, 0.0693	0.0512, 0.1200	0.0432, 0.1007
<i>R</i> ₁ , <i>wR</i> ₂ (all data) ^b	0.0532, 0.1312	0.0848, 0.2169	0.0389, 0.0828	0.0347, 0.0726	0.0662, 0.1305	0.0505, 0.1056

$$^a R_1 = \sum ||F_o| - |F_c|| / \sum |F_o|, \quad ^b wR_2 = \sqrt{\sum w(|F_o|^2 - |F_c|^2)^2} / \sum w(F_o)^2)^{1/2}$$

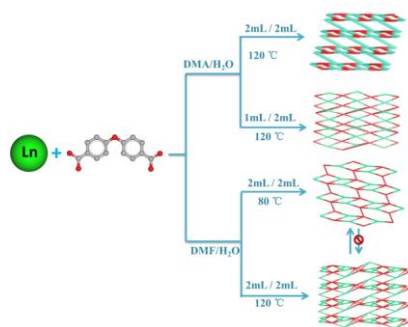
the DMA was replaced by DMF, two additional 2D Ln-MOFs **3** and **4** with structural diversities were harvested.

Infrared spectra

IR spectra data of the organic ligand and the complexes were measured in the range 400–4000 cm⁻¹ (Fig S1). Compared with the free ligand, the $\nu_{C=O}$ (–COOH) of 1683 cm⁻¹ disappears in the IR spectra of the complexes, and the characteristic peaks of $\nu_{as}(\text{COO}^-)$ and $\nu_s(\text{COO}^-)$ are observed at 1596–1598 cm⁻¹ and 1410–1415 cm⁻¹ for **1-4**, respectively. These facts indicate that the carboxylate groups are coordinated to the Ln³⁺ ion¹⁴. Important IR bands of the ligand and Ln-MOFs are listed in Table S1.

PXRD and TG analysis

The phase purities of all Ln-MOFs are demonstrated by X-ray power diffraction analysis at room temperature. The experimental PXRD patterns of as-synthesized samples match well with their simulated spectra based on single-crystal X-ray data, indicating the high purity of all Ln-MOFs (Fig. S2).



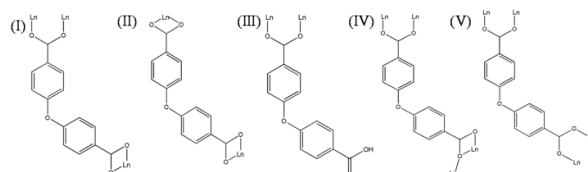
Scheme 2 Synthesis of the Ln-MOFs

To examine the thermal stabilities of these Ln-MOFs, TG analyses were carried out in a nitrogen atmosphere with a heating

rate of 10 °C/min and in the temperature range of 25–800 °C (Fig. S3). The same type of Ln-MOFs show similar weight loss due to their isostructural nature, **1-Tb**, **2-Tb**, **3-Tb**, and **4-Tb** are served as representative to describe the thermal stabilities in detail. The TGA curve of **1-Tb** exhibits a weight loss 15.90% in the range of 25 to 400 °C, corresponding to the escape of two coordinated water molecules and two coordinated DMA molecules (calcd 16.19%). Above 500 °C, a rapid weight loss is observed, which is attributed to the decomposition of the framework. **2-Tb** show a weight loss of 8.64% resulting from removal of four coordinated water molecules and two lattice water molecules (calcd 9.05%) from 25 to 210 °C, and the desolvated framework is stable until 500 °C. **3-Tb** show a rapid weight loss of 24.02% from 25 to 290 °C, due to the removal of three lattice DMF molecules (calcd 23.63%), as temperature continue to rise, the framework decomposed. For **4-Tb**, the first weight loss of 6.59% from 25 to 330 °C, which is attribute to the release of one coordinated DMF molecules (calcd 6.11%), followed by a loss approximately 3.51% from 340 to 450 °C, attributed to removal of two coordinated water molecules (calcd 3.01%).

Crystal structures

There are four types of isostructural Ln-MOFs. **1-Tb**, **2-Tb**, **3-Tb**, and **4-Tb** are served as representative to describe structures in detail. SHAPE software is used to analysis lanthanide geometry. Structural analysis of these Ln-MOFs shows that H₂OBA has five coordination modes (Scheme 3). The structural features of all Ln-MOFs are shown in Table 2.



Scheme 3 Coordination modes of the ligand

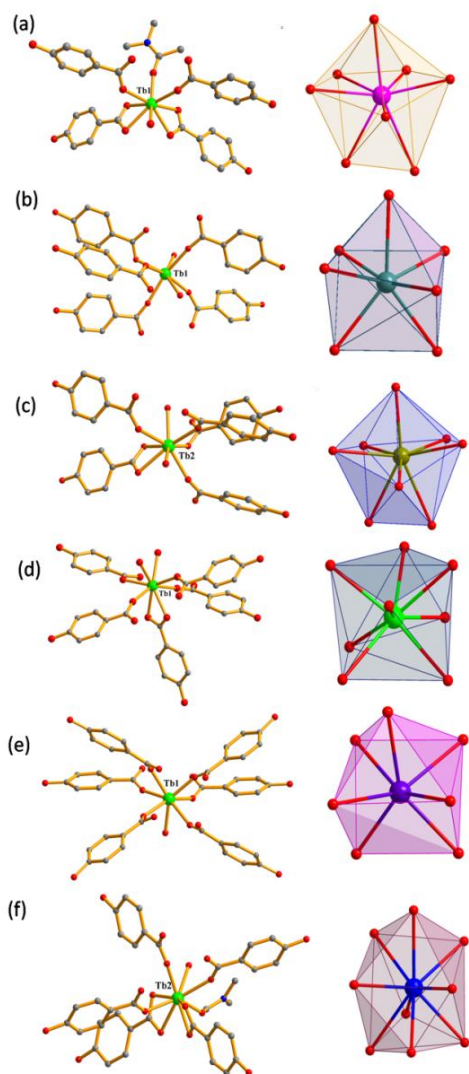
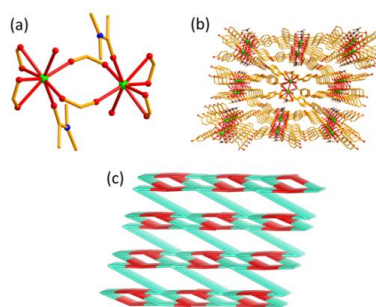


Fig. 1 Coordination environments of **1-4** (hydrogen atoms are omitted for clarity). (a) Coordination environment of Tb1 in **1**. (b) Coordination environment of Tb1 in **2**. (c) Coordination environment of Tb2 in **2**. (d) Coordination environment of Tb1 in **3**. (e) Coordination environment of Tb1 in **4**. (f) Coordination environment of Tb2 in **4**.

Crystal structure of 1-Tb. Single-crystal structure analysis reveals that **1-Tb** crystallizes in the monoclinic crystal system with space group $C2/c$. Its asymmetric unit contains one Tb^{3+} ion, one and a half of OBA^{2-} ligands, one DMA molecule and one water molecule. Tb^{3+} ion is eight-coordinated and surrounded by eight oxygen atoms from four OBA^{2-} ligands, one DMA molecule and one water molecule, forming a D_{2d} triangular dodecahedron geometry (Fig. 1a). The Tb-O bond lengths are in the range of 2.249(7)-2.540(7) Å. The OBA^{2-} ligands have two different coordination modes, namely bidentate bridging and bidentate chelating modes. Two crystallographically equivalent Tb^{3+} ions are bridged by two carboxylate groups to give a dinuclear secondary building units (SBU) (Fig. 2a). The dinuclear SBUs are cross-linked by the OBA^{2-} ligands to form a 3D coordination polymer network (Fig. 2b). Considering ligand as 3-connected node and the Tb^{3+} as 4-connected node, the whole framework can be simplified as a 3,4-connected 2-nodal net topology with a point symbol of $\{4^2.6.12^3\}\{4^2.6\}$ (Fig. 2c).



25

Fig. 2 (a) Dinuclear SBUs in **1-Tb**. (b) Representation of 3D framework of **1-Tb**. (c) Topological view of **1-Tb**.

Crystal structure of 2-Tb. Comprehensive analysis of X-ray power diffraction reveals that Ln-MOFs **2-Eu** and **2-Tb** are isostructural,¹¹ except two additional lattice water molecules. The single-crystal structure of **2** is described briefly. There are two crystallographically independent Ln^{3+} ($Ln1$, $Ln2$) in **2**, forming C_{2v} capped trigonal prism ($Ln1$) and D_{2d} triangular dodecahedron ($Ln2$) geometry, respectively (Fig. 1b and Fig. 1c). Adjacent $Ln1 \cdots Ln1$, $Ln1 \cdots Ln2$, $Ln2 \cdots Ln2$ are alternately arranged by carboxylate of the OBA^{2-} ligands to form a 1D chains (Fig. 3a). The 1D chains are further linked by the OBA^{2-} ligands to get a 2D network (Fig. 3b). Considering ligand as 4-connected node and the Tb1, Tb2 as 4-c and 5-c nodes, The 2D network can be simplified as a 4,4,5-connected 3-nodal net topology with a point symbol of $\{3.4^4.5^3.6^2\}2\{3.4^4.6\}\{4^4.6^2\}$ (Fig. 3c).

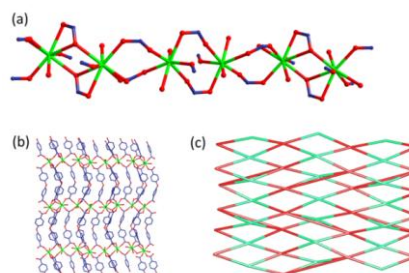


Fig. 3 (a) View of 1D chain bridged by OBA^{2-} ligands in **2**. (b) View of 2D network of **2**. (c) Topological view of **2**.

Crystal structure of 3-Tb. Single-crystal structure analysis reveals that **3-Tb** crystallizes in the triclinic crystal system with space group $P\bar{1}$. The asymmetric unit composes of one crystallographically independent Tb^{3+} ion, one OBA^{2-} ligand, one $HOBA^-$ ligand, two water molecules and three lattice DMF molecules. Tb^{3+} ion is eight-coordinated and surrounded by eight oxygen atoms from five OBA^{2-} ligands and two water molecules, forming a distorted D_{4d} square antiprism geometry (Fig. 1d). The Tb-O bond lengths are in the range of 2.310(2)-2.494(2) Å. Two adjacent Tb^{3+} ions are bridged by two didentate bridging carboxylate groups to form a 1D chain (Fig. 4a). The 1D chains are further connected by the OBA^{2-} ligands to form a 2D coordination polymer network (Fig. 4b). In order to make a better understanding of its structure, the central metal ion and the organic ligand can be simplified as 4-c and 3-c nodes, respectively. These two kinds of nodes form a 3,4-connected 2-nodal net topology with a point symbol of $\{4^2.6^3.8\}\{4^2.6\}$ (Fig. 4c).

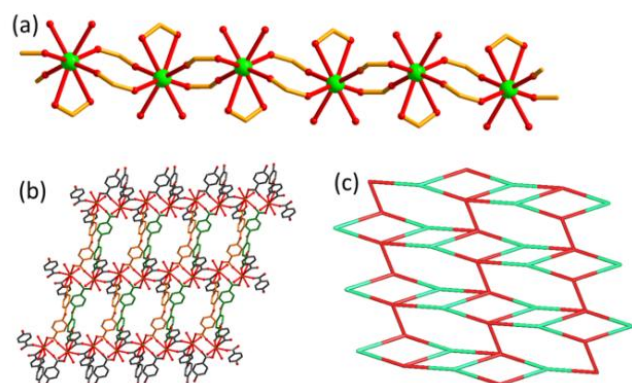


Fig. 4 (a) View of 1D chain bridged by OBA²⁻ ligands in **3-Tb**. (b) View of 2D network of **3-Tb**. (c) Topological view of **3-Tb**.

Crystal structure of 4-Tb. Single-crystal structure analysis reveals that **4-Tb** crystallizes in the monoclinic $P2_1/c$ space group. The asymmetric unit consists of two crystallographically independent Tb³⁺ ions, three OBA²⁻ ligands, two water molecules and one DMF molecule. Tb1 is seven-coordinated and surrounded by seven oxygen atoms from six OBA²⁻ ligands and one water molecule, forming a C_{2v} capped trigonal prism geometry (Fig. 1e). The Tb-O bond lengths are in the range of 2.206(5)-2.507(6) Å. Adjacent Tb1 bridged by four bidentate chelating carboxylate groups to form a dinuclear secondary building unit (SBU) (Fig. 5a). The SBUs are further bridged by two carboxylate groups to generate a 1D chain (Fig. 5c). Tb2 are nine-coordinated and surrounded by nine oxygen atoms from five OBA²⁻ ligands, one water molecule and one DMF molecule, forming a C_s Muffin geometry (Fig. 1f). The Tb-O bond lengths are in the range of 2.145(6)-2.595(7) Å. Adjacent Tb2 bridged by

four bridging carboxylate groups to form another {Tb₂} secondary building unit with a Tb··Tb distance of 3.567(6) Å (Fig. 5b). The OBA²⁻ ligands join the 1D chains and dinuclear {Tb₂} SBUs into a 2D network, in which the 1D chains and the dinuclear {Tb₂} SBUs arranged alternately (Fig. 5d). For further understanding of the topology of **4**, Tb1 and Tb2 can be viewed as 6-connected and 5-connected nodes, and the three different coordination modes of OBA²⁻ considered as 3-connected, 4-connected, 4-connected nodes, respectively. These five kinds of nodes generate a 3,4,4,5,6-connected 5-nodal net topology with a point symbol of {4³}{4⁴.6²}{4⁵.6}{4⁸.6²}{4⁹.6⁴.8²} (Fig. 5e).

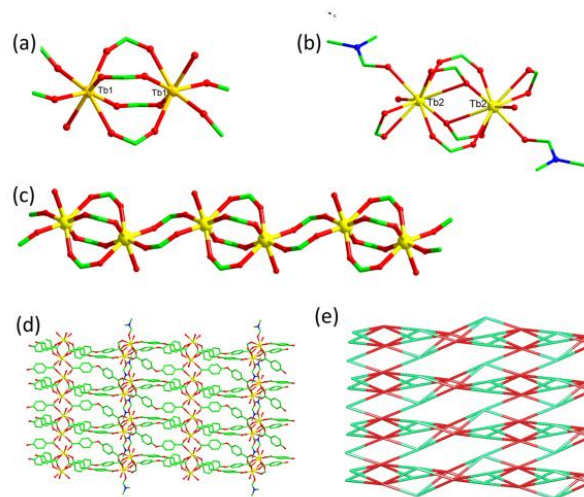


Fig. 5 (a) View of the {Tb₂} dinuclear SBU of Tb1 in **4-Tb**. (b) View of the {Tb₂} dinuclear SBU of Tb2 in **4-Tb**. (c) View of 1D chain form by Tb1 dinuclear SBUs in **4-Tb**. (d) View of 2D network of **4-Tb**. (e) Topological view of **4-Tb**.

Table 2 Comparison of structural features for **1-4**

Ln-MOFs	Space group	Coordination number	Coordination configuration	Coordination modes	Dimensionality
1	$C2/c$	eight	Triangular dodecahedron (D _{2d})	I, II	3D
2	$P2_1/c$	seven, eight	Capped trigonal prism (C _{2v}), Triangular dodecahedron (D _{2d})	IV, V	2D
3	$P\bar{1}$	eight	Triangular dodecahedron (D _{2d})	I, III	2D
4	$P2_1/c$	seven, nine	Capped trigonal prism (C _{2v}), Muffin(C _s)	I, IV, V	2D

Structural transformation from **4** to **3**

Interestingly, when the needle-like crystals of **4** stayed in mother solution at room temperature for two days, block-like crystals of **3** were obtained. This transformation was verified by the PXRD measurement (Fig. S4), indicate that **4** can transform into **3** in mother solution.

The breakage of Tb1-O bonds (2.5070(6) Å, the orange ones) of the {Tb₂} dinuclear SBUs in 1D chain (Fig. 6a) of **4** lead to the breakup of the SBUs and subsequent linked to the adjacent Tb1, the water molecules coordinated to the open metal sites (Fig. 6b), forming a new 1D chain. The removal of DMF molecules of another {Tb₂} SBUs (Fig. 6c) induces the breakup of the SBUs. The breakage of Tb-O bonds (2.539(4) Å, 2.575(5) Å, orange ones) lead to the connection of the adjacent {Tb₂} unit, meanwhile water molecules occupy the metal site (Fig. 6d) and

form 1D Tb-O chain (Fig. 6e).

From **4** to **3**, the coordination geometry of the metal centre changed. In **3**, each OBA²⁻ ligand is bonded to three Tb³⁺ ions and each Tb³⁺ ion is bound to four OBA²⁻ ligand, while in **4**, two kinds of coordination geometry exist, each Tb1 is bound to six OBA²⁻ ligand and each Tb2 is bound to five OBA²⁻ ligand. The Tb··Tb distance of 5.4984(5) Å between two {Tb₂} units of the 1D chain in **4** is reduced to 5.0043(4) Å in **3**, while the Tb··Tb separation within a given {Tb₂} units of the 1D chain increases from 4.0815(4) Å in **4** to 4.5786 (3) Å in **3**. The Tb··Tb distance of 8.5029(6) Å between the other type of two discrete {Tb₂} units in **4** is reduced to 5.0043(4) Å in **3**, while the Tb··Tb separation within a given {Tb₂} units of the 1D chain increases from 3.5673(5) Å in **4** to 4.5786 (3) Å in **3**.

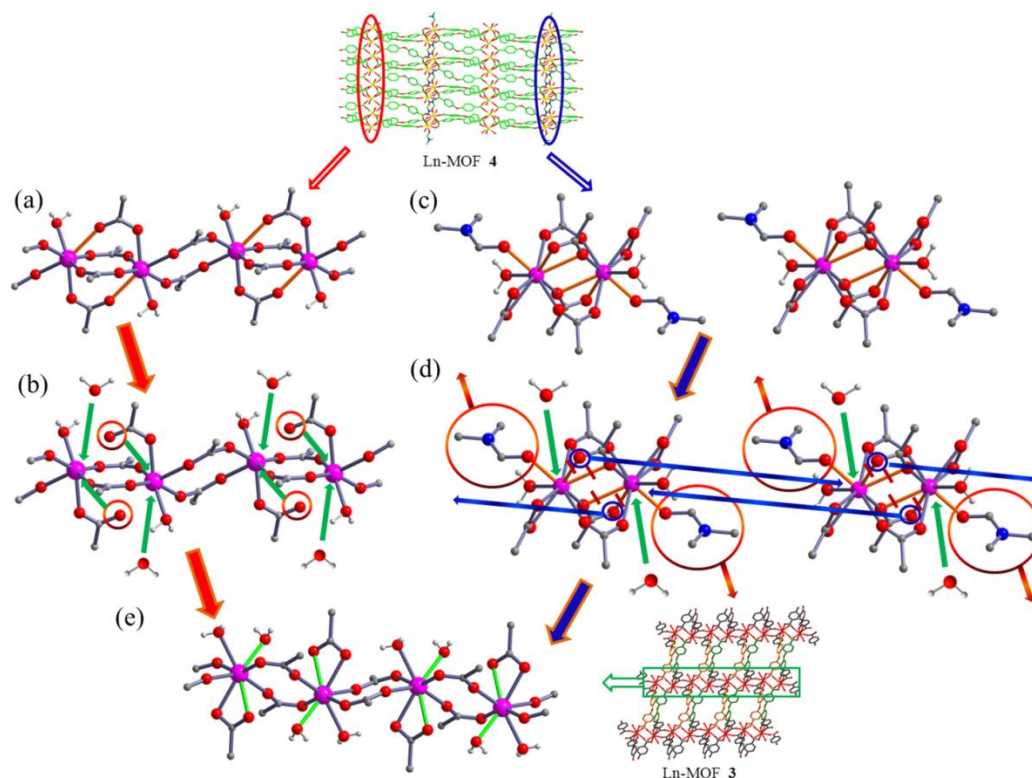


Fig. 6 (a) 1D chains of Tb1 in **4**. (b) Breakage of the Tb-O bonds and the coordination of water molecules. (c) $\{Tb_2\}$ SBUs in **4**. (d) Removal of DMA molecules of $\{Tb_2\}$ SUBs in **4** and a rearrangement of the coordination geometry. (e) The formation of the Tb-O bonds.

Luminescent properties

The solid luminescent spectra of **1-4** were recorded at room temperature (Fig. 7). When illuminated with laboratory UV light at 254 nm, Eu-MOFs (**1-Eu**, **2-Eu**, **3-Eu**, **4-Eu**) and Tb-MOFs (**1-Tb**, **2-Tb**, **3-Tb**, **4-Tb**) display strong green and red fluorescence, respectively. When excited at 300 nm, Eu-MOFs exhibit four characteristic emission bands around 591, 616, 652, and 700 nm coming from $^5D_0 \rightarrow ^7F_J$ ($J=1-4$)¹⁵ transitions of Eu^{3+} ion, respectively. The luminescent spectra of Eu-MOFs show two main emission bands at 591 and 616 nm. The strongest emission at 616 nm in the red region is attributed to $^5D_0 \rightarrow ^7F_2$ transitions. The dominated $^5D_0 \rightarrow ^7F_2$ transition is an electron dipole transition, the so-called hypersensitive transition, which is responsible for the visible brilliant red emission of Eu-MOFs. Excitation of Tb-MOFs at 300 nm show four characteristic emission bands of 488, 545, 583, and 621 nm assigned to $^5D_4 \rightarrow ^7F_J$ ($J=6-3$) transitions of Tb^{3+} ion.¹⁶ The spectrum is dominated by $^5D_4 \rightarrow ^7F_3$ transition at 545 nm, which determines the green luminescence of the Tb-MOFs.

Conclusions

In summary, we have successfully synthesized four types of Ln-MOFs based on a V-shaped ligand 4,4'-oxybis(benzoate) acid by controlling of reaction conditions, which show interesting diversity. The diversity of the structures reveals that solvent and temperature play important roles in constructing coordination polymers. This work may give new insights into the design, construction and modification of functional Ln-MOFs towards specified applications.

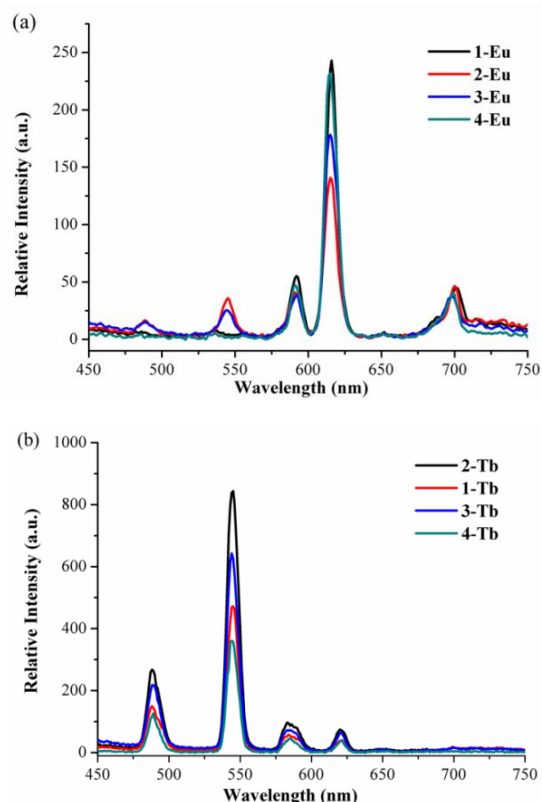


Fig. 7 Emission spectra of Eu-MOFs (a) and Tb-MOFs (b) in the solid state at room temperature.

Acknowledgements

This work was supported by NSFC (21421001), the MOE (IRT-13022, 13R30), 111 project (B12015), the NSF of Tianjin (13JCZDJC32200).

Notes and references

⁵ Department of Chemistry, Key Laboratory of Advanced Energy Material Chemistry (MOE), and Collaborative Innovation Center of Chemical Science and Engineering (Tianjin), Nankai University, Tianjin 300071, P. R. China. Fax: (+86)22-23502458; E-mail: pcheng@nankai.edu.cn.

¹⁰ † Electronic Supplementary Information (ESI) available: PXRD data, TGA data. CCDC1030082-1030087. See DOI:10.1039/b000000x/

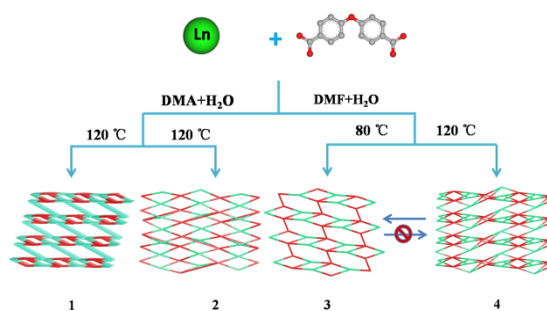
- 1 (a) P. Cheng (Ed.) "Lanthanide Metal-Organic Frameworks", Struct Bond, Springer, 2014, DOI 10.1007/978-3-662-45773-3. (b) Y. He, H. Furukawa, C. Wu, M. O'Keeffe, R. Krishna and B. Chen, *Chem. Commun.*, 2013, **49**, 6773–6775; (c) H. He, D. Yuan, H. Ma, D. Sun, G. Zhang and H.-C. Zhou, *Inorg. Chem.*, 2010, **49**, 7605–7607; (d) J.-J. Jiang, M. Pan, J.-M. Liu, W. Wang and C.-Y. Su, *Inorg. Chem.*, 2010, **49**, 10166–10173; (e) J.-R. Li, R. J. Kuppler and H.-C. Zhou, *Chem. Soc. Rev.*, 2009, **38**, 1477–1504; (f) L. Pan, K. M. Adams, H. E. Hernandez, X. Wang, C. Zheng, Y. Hattori and K. Kaneko, *J. Am. Chem. Soc.*, 2003, **125**, 3062–3067; (g) Z. Guo, H. Xu, S. Su, J. Cai, S. Dang, S. Xiang, G. Qian, H. Zhang, M. O'Keeffe and B. Chen, *Chem. Commun.*, 2011, **47**, 5551–5553.
- 2 (a) A. U. Czaja, N. Trukhan and U. Mueller, *Chem. Soc. Rev.*, 2009, **38**, 1284–1293; (b) D. Dang, Y. Bai, C. He, J. Wang, C. Duan and J. Niu, *Inorg. Chem.*, 2010, **49**, 1280–1282; (c) R. F. D'Vries, M. Iglesias, N. Snejko, E. Gutierrez-Puebla and M. Angeles Monge, *Inorg. Chem.*, 2012, **51**, 11349–11355; (d) Y. Liu, K. Mo and Y. Cui, *Inorg. Chem.*, 2013, **52**, 10286–10291; (e) L. Ma, C. Abney and W. Lin, *Chem. Soc. Rev.*, 2009, **38**, 1248–1256; (f) N. Wei, M.-Y. Zhang, X.-N. Zhang, G.-M. Li, X.-D. Zhang and Z.-B. Han, *Cryst. Growth Des.*, 2014, **14**, 3002–3009.
- 3 (a) M. D. Allendorf, C. A. Bauer, R. K. Bhakta and R. J. T. Houk, *Chem. Soc. Rev.*, 2009, **38**, 1330–1352; (b) J. Rocha, L. D. Carlos, F. A. Almeida Paz and D. Ananias, *Chem. Soc. Rev.*, 2011, **40**, 926–940; (c) M. Zhu, Z.-M. Hao, X.-Z. Song, X. Meng, S.-N. Zhao, S.-Y. Song and H.-J. Zhang, *Chem. Commun.*, 2014, **50**, 1912–1914; (d) J. C. Rybak, L. V. Meyer, J. Wagenhoefer, G. SEXTL and K. Mueller-Buschbaum, *Inorg. Chem.*, 2012, **51**, 13204–13213; (e) J.-M. Zhou, W. Shi, H.-M. Li, H. Li, and P. Cheng, *J. Phys. Chem., C* 2014, **118**, 416–426; (f) J.-M. Zhou, W. Shi, N. Xu, and P. Cheng, *Inorg. Chem.*, 2013, **52**, 8082–8090.
- 4 (a) L.-X. Chang, G. Xiong, L. Wang, P. Cheng and B. Zhao, *Chem. Commun.*, 2013, **49**, 1055–1057; (b) S. Biswas, H. S. Jena, A. Adhikary and S. Konar, *Inorg. Chem.*, 2014, **53**, 3926–3928; (c) S. Mohapatra, B. Rajeswaran, A. Chakraborty, A. Sundaresan and T. K. Maji, *Chem. Mater.*, 2013, **25**, 1673–1679; (d) S. Zhang, W. Shi, L. Li, E. Duan, and P. Cheng, *Inorg. Chem.*, 2014, **53**, 10340–10346; (e) L. Tian, Y.-Q. Sun, B. Na, and P. Cheng, *Eur. J. Inorg. Chem.*, 2013, 4329–4335.
- 5 (a) A. Bourdolle, M. Allali, J. C. Mulatier, B. Le Guennic, J. M. Zwiier, P. L. Baldeck, J. C. G. Bunzli, C. Andraud, L. Lamarque and O. Maury, *Inorg. Chem.*, 2011, **50**, 4987–4999; (b) B. Chen, L. Wang, F. Zapata, G. Qian and E. B. Lobkovsky, *J. Am. Chem. Soc.* 2008, **130**, 6718.
- 6 (a) F. S. Richardson, *Chem. Rev.* 1982, **82**, 541–552; (b) G. F. Sáde, O. L. Malta, C. de Mello Donegáde, A. M. Simas, R. L. Longo, P. A. Santa-Cruz and E. F. da Silva Jr, *Coord. Chem. Rev.* 2000, **196**, 165–195.
- 7 (a) A. Nag, M. V. Kovalenko, J. S. Lee, W. Y. Liu, B. Spokoyny and D. V. Talapin, *J. Am. Chem. Soc.*, 2011, **133**, 10612–10620; (b) J. Zhang, B. Zheng, T. Zhao, G. Li, Q. Huo and Y. Liu, *Cryst. Growth Des.*, 2014, **14**, 2394–2400.
- 8 (a) N. Stock and S. Biswas, *Chem. Rev.*, 2012, **112**, 933–969; (b) X.-Q. Song, Y.-K. Lei, X.-R. Wang, M.-M. Zhao, Y.-Q. Peng and G.-Q. Cheng, *J. Solid State Chem.*, 2014, **218**, 202–212.

- 9 (a) W.-G. Lu, D.-C. Zhong, L. Jiang and T.-B. Lu, *Cryst. Growth Des.*, 2012, **12**, 3675–3683; (b) P. J. Saines, M. Steinmann, J.-C. Tan, H. H.-M. Yeunga, and A. K. Cheetham, *CrystEngComm.*, 2013, **15**, 100–110; (c) G.-G. Gao, C.-Y. Song, X.-M. Zong, D.-F. Chai, H. Liu, Y.-L. Zou, J.-X. Liu and Y.-F. Qiu, *CrystEngComm.*, 2014, **16**, 5150–5158; (d) S.-J. Wang, Y.-W. Tian, L.-X. You, F. Ding, K. W. Meert, D. Poelman, P. F. Smet, B.-Y. Ren and Y.-G. Sun, *Dalton Trans.*, 2014, **43**, 3462–3470; (e) Q.-Y. Liu, W.-F. Wang, Y.-L. Wang, Z.-M. Shan, M.-S. Wang and J. Tang, *Inorg. Chem.*, 2012, **51**, 2381–2392.
- 10 Y.-W. Lin, B.-R. Jian, S.-C. Huang, C.-H. Huang and K.-F. Hsu, *Inorg. Chem.*, 2010, **49**, 2316.
- 11 Y.-B. Wang, C.-Y. Sun, X.-J. Zheng, S. Gao, S.-Z. Lu and L.-P. Jin, *Polyhedron*, 2005, **24**, 823.
- 12 G. F. Liu, Z. P. Qiao, H. Z. Wang, X. M. Chen and G. Yang, *New J. Chem.*, 2002, **26**, 791.
- 13 (a) G. M. Sheldrick, SHELXL-97, Program for Crystal Structure Refinement; University of Göttingen: Göttingen, Germany, 1997; (b) G. M. Sheldrick, SHELXS-97, Program for Crystal Structure Solution; University of Göttingen: Göttingen, Germany, 1997.
- 14 (a) Y.-Z. Shi, X.-Z. Sun and Y.-H. Jiang, Spectra and Chemical Identification of Organic Compounds, Science and Technology Press, Nanjing, 1988, p. 98; (b) H.-M. Ye, N. Ren, J.-J. Zhang, S.-J. Sun and J.-F. Wang, *New J. Chem.*, 2010, **34**, 533.
- 15 (a) A. de Bettencourt-Dias and S. Viswanathan, *Chem. Commun.* 2004, 1024–1025; (b) Y. Q. Sun, J. Zhang, Y. M. Chen and G. Y. Yang, *Angew. Chem., Int. Ed.*, 2005, **44**, 5814–5817; (c) G. Vicentini, L. B. Zinner, J. Zukerman-Schpector and K. Zinner, *Coord. Chem. Rev.*, 2000, **196**, 353–382.
- 16 (a) Z.-J. Lin, B. Xu, T.-F. Liu, M.-N. Cao, J. Lü and R. Cao, *Eur. J. Inorg. Chem.*, 2010, 3842–3849; (b) C. Tedeschi, J. Azóna, H. Gornitzka, P. Tisnès and C. Picard, *Dalton Trans.*, 2003, 1738–1745.

For Table of Contents Use Only

Structural Diversity of Luminescent Lanthanide Metal-Organic Frameworks based on a V-Shaped Ligand

Yan-Fei He, Di-Ming Chen, Hang Xu and Peng Cheng*



A systematic research of solvent and temperature induced structural diversity of lanthanide Metal-Organic Frameworks based on a V-Shaped Ligand.